Field emission of carbon nanotube array with normal-gate cold cathode*

Dai Jian-Feng(戴剑锋)[a)b)†], Mu Xiao-Wen(慕晓文)[b)], Qiao Xian-Wu(乔宪武)[b)], Chen Xiao-Ting(陈小婷)[b)], and Wang Jun-Hong(王军红)[b)]

[a)] *State Key Laboratory of Gansu Advanced Non-Ferrous Metal Materials, Lanzhou University of Technology, Lanzhou* 730050, *China*
[b)] *School of Science, Lanzhou University of Technology, Lanzhou* 730050, *China*

(Received 6 November 2009; revised manuscript received 1 December 2009)

A hexagon pitch carbon nanotube (CNT) array vertical to the normal gate of cold cathode field emission displayer (FED) is simulated by solving the Laplace equation. The calculated results show that the normal gate causes the electric field around the CNT tops to be concentrated and the emission electron beam becomes a column. The field enhancement factor and the emission current intensity step up greatly compared with those of the diode structure. Emission current density increases rapidly with the decrease of normal-gate aperture. The gate voltage exerts a critical influence on the emission current.

Keywords: field emission, hexagon pitch carbon nanotube (CNT) array, emission current density, field enhancement factor

PACC: 7210, 7220H, 7970

1. Introduction

Owing to unique mechanical and electrical properties, thermal stability and excellent structure, carbon nanotubes (CNTs) are certainly one of the most exciting discoveries in nanotechnology.[1−4] It is well known that compared with other field emitters, the CNT emitter has many unique properties such as great aspect ratio, small work function and high conductivity, which lead CNTs to possess the following features: high current density, low threshold voltage and ultrahigh field enhancement factor. The enhancement factor and the electric field distribution of the CNT field emission displayer (CNT-FED) device can be influenced by aspect ratio, anode–cathode distance, density of CNT array, CNT array geometry, CNT structure and so on.[5−9] Compared with the square array, the hexagon array is more stable and available. Thus, the CNT array, plumbed with hexagon pitch arrangement on the normal-gate cold cathode, has a CNT-FED structure with the highest prospect of application. The nanoscale tip and the higher aspect ratio would lead to such a large local field at the tip of CNT that the emission electrons could penetrate through the potential barrier and enter into the vacuum by tunnel effect,[10] thereby achieving a higher current density at a lower voltage. High current density and ultrahigh field enhancement factors are essential to the field emission. The aligned CNTs with a more excellent field emission property and ultrahigh field enhancement factor were achieved readily.[11] Therefore, it is not surprising that CNT is considered to be an ideal candidate for the next generation of field emitters.[12,13] Recently, lots of researches on the field emission of CNT-FED with diode structure have been conducted.[3−9,12−14] However, researches about CNT-FED with normal-gate are rare, and the mechanism of field emission with using a CNT array as an emitter is still not fully clear. The further modeling and calculation based on the field emission from the CNTs array are required. Usually there are two methods, i.e. the floating charge sphere method and solving the Laplace equation method, which have been used to simulate the CNT-FED at present.[14−16] Generally speaking, the floating charge sphere method is suited to dot charge, but it cannot be used to depict the distribution of the electric field and potential in CNT array. Although it is difficult to solve the solving

*Project supported by the National Natural Science Foundation of China (Grant No. 50873047), and the Foundation of Gansu Provincial Education Department, China (Grant No. 0603-02).
†Corresponding author. E-mail: jfdai1963@sohu.com
© 2010 Chinese Physical Society and IOP Publishing Ltd

Laplace equation, the electric field and the potential distribution of CNT array in the whole space, and the field enhancement factors in various cases can be obtained. The CNT array plumbed with hexagon pitch arrangement on the normal-gate of cold cathode has been established and analysed by solving the Laplace equation. The results indicate that the electric field at the apexes of CNTs increases critically and concentrates in normal-gate structure compared with those in diode structure. Normal-gate aperture has a critical influence on emission current intensity, which is increased rapidly by reducing the normal-gate aperture. Thus a higher field enhancement factor can be achieved than in the case without the normal gate. A higher gate voltage exerts a great influence on the emission current density.

2. Modeling and calculations

The structure of CNT-FED with normal gate of cold cathode is shown in Fig. 1, in which the anode is made of transparent conductive Indium Tin Oxides (ITO) film, and its surface is coated with phosphor. CNTs are in hexagon pitch arrangement, standing perpendicularly on the cathode plane, with height L, and they are closed with a hemispherical cap with radius r_0. The normal gate is made of Al film of a thickness $d_{\rm g} = 50$ nm which is deposited on an insulating layer. Normal gate connects with anode and cathode by insulating pillar made of polymethylmethacrylate (PMMA) and silicon dioxide (SiO_2) insulating layer respectively. The anode, the cathode, and the normal gate connect with an external drive circuit by their own down-lead respectively. The symbols $c, R, d_{\rm cg}$, $d_{\rm ag}$ and $d_{\rm g}$ represent the intertube distance, the radius of gate hole, the distances of normal gate to cathode and anode, the thickness of normal gate respectively. Based on some experimental results and its feasibility,[17,18] an FED with a gate-hole radius of 200 nm is easy to achieve. Parameters $c = 50$ nm, $R = 200$ nm, $d_{\rm cg} = 30$ μm, $d_{\rm ag} = 80$ μm, $d_{\rm g} = 50$ nm, $r_0 = 10$ nm, $L = 60$ μm, $V_{\rm a} = 2000$ V, and $V_{\rm g} = 100$ V are adopted in this model. CNT with a radius of 10 nm is known as multi-wall carbon nanotube (MWCNT), and the MWCNT are metallic,[14] so the potential is maintained to be zero over the whole CNTs.

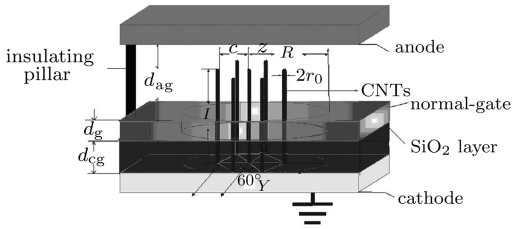


Fig. 1. Modeling for CNT-FED with normal-gate cold cathode.

The potential of the CNTs can be described by solving the Laplace equation ($\nabla^2\phi = 0$). Considering its symmetry, the expression of potential ϕ can be expressed as

$$\frac{\partial^2\phi}{\partial z^2} + \frac{1}{r}\frac{\partial\phi}{\partial r} + \frac{\partial^2\phi}{\partial r^2} = 0, \tag{1}$$

which is consistent with the former conclusion.[19]

The initial and boundary conditions can be expressed as

$$\phi|_{z=0} = 0, \quad \phi|_{z=d_{\rm ag}+d_{\rm cg}+d_{\rm g}} = V_{\rm a},$$

$$\phi|^{r=R}_{z=d_{\rm cg}+d_{\rm g}} = V_{\rm g}, \quad \phi|_{z=L,0\le r\le r_0} = 0,$$

and

$$\phi|_{r=r_0,0\le Z\le L} = 0.$$

As a result,

$$\begin{aligned}\phi(z,r) &= V_{\rm g} + (V_{\rm a} - V_{\rm g})\frac{(z-d_{\rm cg})}{d_{\rm ag}} \\ &\quad - \frac{V_{\rm g}d_{\rm ag} + (V_{\rm a}-V_{\rm g})(z-d_{\rm cg})}{d_{\rm ag}N_0(k_1r_0)}N_0(k_1r).\end{aligned} \tag{2}$$

For a CNT array with hexagon pitch arrangement, the potential and the electric field can be described as follows:

$$\begin{aligned}\phi_{\rm A} &= 7V_{\rm g} + 7(V_{\rm a}-V_{\rm g})\frac{(z-d_{\rm cg})}{d_{\rm ag}} - \frac{V_{\rm g}d_{\rm ag} + (V_{\rm a}-V_{\rm g})(z-d_{\rm cg})}{d_{\rm ag}N_0(k_1r_0)}(N_0(k_1r) + 2N_0(k\sqrt{r^2+c^2+rc}) \\ &\quad + 2N_0(k\sqrt{r^2+c^2-rc}) + N_0(k(r+c)) + N_0(k(c-r))), \\ E_{\rm r} &= \frac{V_{\rm g}d_{\rm ag} + (V_{\rm a}-V_{\rm g})(z-d_{\rm cg})}{d_{\rm ag}N_0(k_1r_0)}k_1[N_1(kr) + N_1\left(k\frac{2r+c}{r^2+c^2+rc}\right)\end{aligned} \tag{3}$$

$$+ N_1\left(k\frac{2r-c}{r^2+c^2-rc}\right) + N_1(k(r+c)) - N_1(k(c-r))], \tag{4}$$

$$E_z = -7\frac{V_a - V_g}{d_{ag}} + \frac{(V_a - V_g)}{d_{ag}N_0(k_1 r_0)}((N_0(k_1 r) + 2N_0(k\sqrt{r^2+c^2+rc}) + 2N_0(k\sqrt{r^2+c^2-rc}) + N_0(k(r+c)) + N_0(k(c-r))). \tag{5}$$

Enhancement factor β can be expressed as

$$\beta = \sqrt{\left(\frac{E_r}{E_0}\right)^2 + \left(\frac{E_z}{E_0}\right)^2} = \sqrt{\beta_1^2 + \beta_2^2}, \quad \left(E_0 = \frac{V_a - V_g}{d_{ag}}\right). \tag{6}$$

3. Results and discussion

3.1. Electric field property of CNT array

The electric field distribution of CNT array is given in Fig. 2. The results indicate that the electric field concentrates on the tops of the CNTs, owing to the influence of normal-gate, which means a large number of electrons accumulated there, and produce a partial electric field. According to the calculated result, a strong electric field can be produced at the apexes of CNTs, drops abruptly with radial distance increasing from CNTs, becomes very weak (only about one percent of top's while the radial distance from CNTs is equivalent to about $2.5r_0$). The potential above the apexes of CNTs increases rapidly with the increase of the distance from the local place to CNTs' tops. A great number of electrons are emitted from the tops of CNTs due to the very strong electric field, arrive at the anode plane and illumine the phosphor. This is the reason why CNTs have a lower threshold voltage in field emission. CNTs with a higher aspect ratio could bring about a stronger electric field at the tops.

3.2. Relations between β and V_g for different values of gate-hole radius R

FED with normal-gate cold cathode structure is superior to diode structure. A large number of electrons could be emitted from the cold cathode due to a strong electric field in FED.[19] The total emission current and the number of electrons impinging on the anode layer can be controlled easily by adjusting the gate voltage. The curves for enhancement factor β versus gate voltage with different values of gate radius R are shown in Fig. 3. It can be seen from this figure that the field enhancement factor decreases with the increase of R, and slightly changes when $R = 5$ μm. In other words, the normal gate has little influence on field emission when $R/r_0 \approx 500$. The enhancement factor β of normal-gate structure increases fivefold as compared with that for the diode structure.[20] The gate voltage V_g has a critical influence on enhancement factor β. When $V_g < 85$ V, β grows slowly with the increase of V_g, and when $V_g > 85$ V, the field enhancement factor β increases rapidly and is close to 5000 while $V_g = 100$ V at $R = 0.2$ μm.

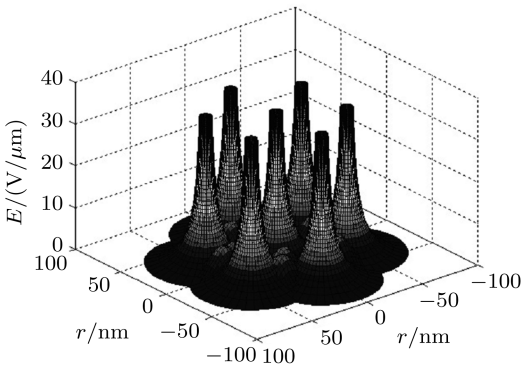


Fig. 2. Electric field distribution of CNT array.

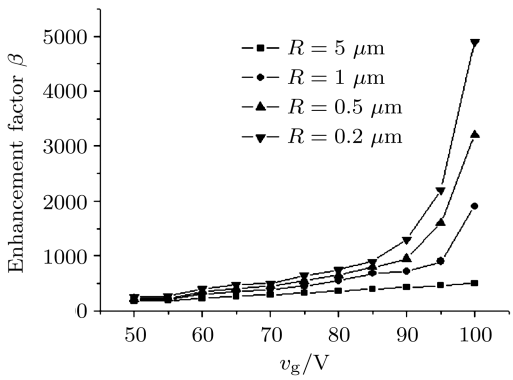


Fig. 3. Influence of gate aperture R on enhancement factor β.

3.3. Variation of J versus V_g and d

The single CNT is analysed by the Fowler–Nordheim (F–N) plot from the following equation:

$$J_s = a\phi^{-1}E^2 \exp\left[\frac{-b\phi^{3/2}}{E}\right],$$

where J_s is the emission current density (in $A \cdot cm^{-2}$), $\phi = 5$ eV is the work function for CNT in the films, E is the excite electric field, a and b are the universal constants: $a = 1.54 \times 10^{-6}$ (in $A \cdot eV \cdot V^{-2}$) and $b = 6.83 \times 10^7$ (in $V \cdot eV^{-3/2} \cdot cm^{-1}$). For the CNT array in hexagon pitch, its emission current density J can be expressed as $J = 2\sqrt{3}J_s/3c^2$, where c is the distance between two neighbouring CNTs. It can be seen clearly from Fig. 4 that the higher the gate voltage is, the larger the emission current will be, thereby exciting a bigger β, which is consistent with the previous experimental results.[21,22]

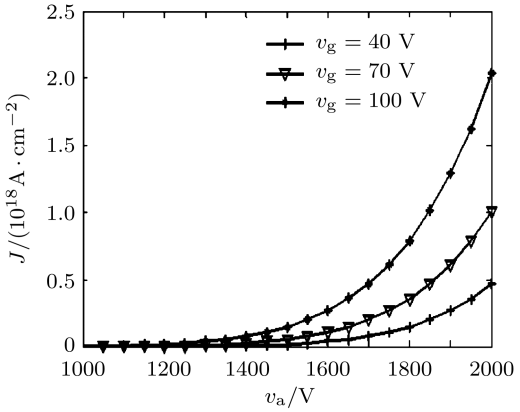


Fig. 4. Emission current density J from CNT array versus the anode voltage V_a.

The current densities of triode and diode structures versus local electric field are shown in Fig. 5. Curve a is for the diode structure cited from Ref. [23] and b is for the normal-gate structure. It can be seen from Fig. 5 that the occurrence of normal-gate leads the emission current density to increase to 10^{15} compared with that of the diode structure. It can be concluded that the FED with normal gate cold cathode structure is superior to diode structure.

The influence of anode–cathode distance on emission current density J is shown in Fig. 6 on condition that $z = 40$ μm, $z = 50$ μm, $z = 60$ μm and $L = 60$ μm. Figure 5 shows that the emission current density J is very sensitive to both d and z, where $d = d_{ag} + d_{cg} + d_g$ is the anode–cathode distance. It is notable that the emission current density reaches a maximal value at a certain distance of anode–cathode, which is about 60 μm here, roughly equal to the length of the tube, this accords with the conclusion in Ref. [24]. The emission current density depends on anode–cathode distance and the distance between anode plate and CNTs' tip separately as shown in Fig. 6. This can be understood by the fact that the rapid increase of electric field with the decrease of z leads to the increase of emission current density.

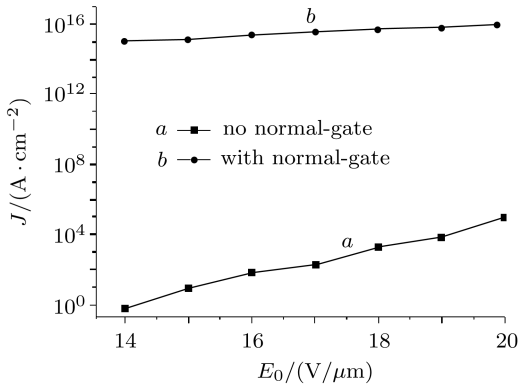


Fig. 5. Emission current density of CNT-FED with normal gate and that of diode structure versus local electric field.

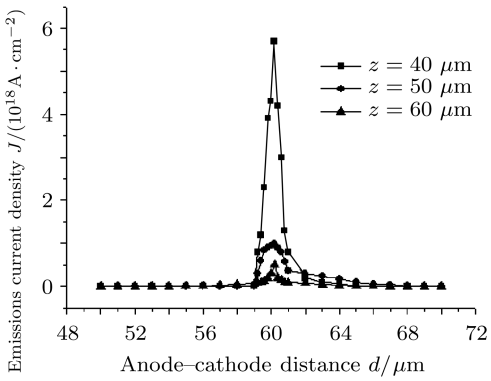


Fig. 6. Curves for emission current density J and distance of anode-cathode d.

4. Conclusion

The model of the CNT array plumbed with hexagon pitch arrangement on the normal-gate of cold cathode is established and analysed. Compared with the diode structure, in the normal-gate structure the electric field concentrates and increases near the tops of the CNTs, the emitted electron beam is shaped into

a column, and the field enhancement factor increases. Emission current intensity increases critically compared with that of the diode structure and increases with normal-gate aperture decreasing. A large emission current can be achieved by increasing the gate voltage. Due to an ultrahigh aspect ratio, small work function, lower threshold voltage and excellent field emission property, the CNT-FED with normal gate could be a more competitive candidate in the FED field.

References

[1] de Heer W A, Chatelain A and Ugrate D 1995 *Science* **270** 1179

[2] Jonge N D, Lamy Y and Schoots K 2002 *Nature* **420** 393

[3] Wang Q H, Corrigan T D and Dai J Y 1997 *Appl. Phys. Lett.* **70** 3308

[4] Wang Y M, Kang W P and Davidson J L 2005 *Diam. Relat. Mater.* **14** 2078

[5] Jung J E, Jin Y W and Choi J H 2002 *Phys. Rev.* B **323** 71

[6] Kim J M, Choi W B and Lee N S 2000 *Diam. Relat. Mater.* **9** 1184

[7] Kimd, Lim S H and Guilley A J 2008 *Thin Solid Films* **516** 706

[8] Lobo T, Figueira M S and Latgee A 2006 *Physica* B **384** 113

[9] Luo M, Wang X Q, Ge H L, Wang M, Xu Y B, Chen Q, Li L P, Chen L, Guan G F, Xia J and Jiang F 2006 *Acta Phys. Sin.* **55** 6063 (in Chinese)

[10] Buldum A and Lu J P 2003 *Appl. Surf. Sci.* **219** 123

[11] Dai J F, Zhang C, Wang Q, Li W X and Yao D 2008 *New Carbon Materials* (Chinese) **23(3)** 201

[12] Wang X Q, Wang M and Li Z H, Yang Bg, Wang F F, He P M and Xu Y B 2005 *Ultramicroscopy* **102** 181

[13] Wang X Q, Wang M and Ge H L 2005 *Physica* E **30** 101

[14] Filip V, Nicolaescu D and Tanemura M 2001 *Ultramicroscopy* **89** 39

[15] Glukhova O E, Zhbanov A I and Torgashov I G 2003 *Appl. Surf. Sci.* **215** 149

[16] Wang M, Shang X F and Li Z H 2006 *Acta Phys. Sin.* **55** 797 (in Chinese)

[17] Shunjiro Fujii, Shin-ichi Honda and Hideyasu Kawai 2008 *Diam. Relat. Mater.* **17** 556

[18] Li Y M and Ta-Ching Yeh 2008 *Comput. Electron.* **7** 332

[19] Lei D, Zeng L Y, Xia Y X, Chen S, Liang J Q and Wang W B 2007 *Acta Phys. Sin.* **56** 6616

[20] Wang X Q, Li L, Chu N J, Jin H X and Ge H L 2008 *Acta Phys. Sin.* **57** 7173

[21] Zhong X F, Yi H C and Wang B P 2004 *Journal of Southeast University* **34** 22

[22] Lu Z L, Wang C Q and Jia Y 2007 *Chin. Phys.* **16** 843

[23] Roy Mahapatra D, Sinha N, Yeow J T W and Melnik R 2008 *Appl. Surf. Sci.* **255** 1959

[24] Chen G H, Wang W L, Peng J, He C S, Deng S Z, Xu N S and Li Z B 2007 *Phys. Rev.* B **76** 195412